JBC Papers in Press. Published on May 23, 2017 as Manuscript M117.789511
The latest version is at http://www.jbc.org/cgi/doi/10.1074/jbc.M117.789511

In silico and cell-based analyses reveal strong divergence between prediction and observation of T cell–recognized tumor antigen T cell epitopes

Julien Schmidt[1], Philippe Guillaume[1], Danijel Dojcinovic[1,†], Julia Karbach[2], George Coukos[1,3] and Immanuel Luescher[1]

From the [1]Ludwig Institute for Cancer Research, University of Lausanne, 1066 Epalinges, Switzerland, [2]Krankenhaus Nordwest, 60488 Frankfurt, Germany, [3]Department of Oncology, University Hospital of Lausanne (CHUV), 1011 Lausanne, Switzerland. [†]Present address: Covance Central Laboratory Services Sarl; 1217 Meyrin, Switzerland

Running title: Identification of cancer T cell epitopes

To whom correspondence should be addressed: Immanuel F. Luescher, PhD, 155 Chemin des Boveresses, 1066 Epalinges, Switzerland, Phone: +41 21 692 5988, E-mail: immanuel.luescher@unil.ch

Keywords: Cancer therapy; major histocompatibility complex (MHC); T cell; transgenic mice; tumor immunology; epitope mapping; viral protein; T cell receptor (TCR).

ABSTRACT

Tumor exomes provide comprehensive information on mutated, over-expressed genes and aberrant splicing, which can be exploited for personalized cancer immunotherapy. Of particular interest are mutated tumor antigen T-cell epitopes, because neoepitope-specific T cells often are tumoricidal. However, identifying tumor-specific T-cell epitopes is a major challenge. A widely used strategy relies on initial prediction of human leukocyte antigen–binding peptides by *in silico* algorithms, but the predictive power of this approach is unclear. Here, we used the human tumor antigen NY-ESO-1 (ESO) and the human leukocyte antigen variant HLA-A*0201 (A2) as a model and predicted *in silico* the 41 highest-affinity, A2-binding 8–11mer peptides and assessed their binding, kinetic complex stability, and immunogenicity in A2-transgenic mice and on peripheral blood mononuclear cells from ESO-vaccinated melanoma patients. We found that nineteen of the peptides strongly bound to A2, ten of which formed stable A2-peptide complexes and induced $CD8^+$ T cells in A2-transgenic mice. However, only five of the peptides induced cognate T cells in humans; these peptides exhibited strong binding and complex stability and contained multiple large hydrophobic and aromatic amino acids. These results were not predicted by *in silico* algorithms and provide new clues to improving T-cell epitope identification. In conclusion, our findings indicate that only a small fraction of *in silico*–predicted A2-binding ESO peptides are immunogenic in humans, namely those that have high peptide-binding strength and complex stability. This observation highlights the need for improving *in silico* predictions of peptide immunogenicity.

Tumor exome and transcriptome sequences provide comprehensive information on mutated, over-expressed genes and aberrant splicing, which can be exploited for cancer immunotherapy. Of special interest are tumor antigen (TA) T cell epitopes containing mutation(s), because neoepitope-specific T cells often are tumoricidal (1,2). To identify TA derived T cell epitopes, MHC binding peptides are usually identified first. To this end MHC-peptide (pMHC) complexes can be isolated from tumor cells and their peptide cargo sequenced by mass spectrometry (3,4). Alternatively *in silico* peptide predictions and peptide binding validation are used (5). Modern *in silico* peptide predictions involve machine-learning techniques like artificial neural networks (ANN) (6). A challenge in peptide prediction is the high diversity of human leucocyte antigens (HLA) alleles; even comprehensive databases, such as IEDB, contain no or limited data for rare alleles, which compromises training of

prediction algorithms (7,8). To improve prediction accuracy pan prediction servers, like NetMHCpan or PickPocket, were introduced that exploit similarities between MHC alleles and their ligand binding properties (9-11). Another difficulty is that MHC class I molecules present peptides of different lengths, usually 8 to 11 residues long. Gapped sequence alignments were introduced to improve predictions of peptide of different length (9,12,13). By including proteasomal cleavage predictions peptide prediction accuracy can be further increased (8,14). Different *in silico* MHC ligand prediction algorithms can be combined to reduce the number of peptide candidates (8,15).

Only a small fraction of HLA ligands is immunogenic and *in silico* prediction of these is challenging due to ambiguities of prediction parameters. According to some studies immunogenicity correlates with peptide binding affinity (5), pMHC complex kinetic stability (16) or both (17). Moreover, it has been reported that immunogenic peptides contain large aliphatic and/or aromatic residues in TCR accessible positions (18,19). T cell epitope prediction servers like NetTepi or IEDB immunogenicity integrate such parameters (18,20). However, peptide's immunogenicity depends also on other factors, such as the efficiency of their production and presentation by professional antigen presenting cells (APC) and on central tolerance (1,2). For personalized cancer immunotherapy it is crucial to identify TA-specific T cell epitopes and available procedures are error prone (21).

To identify key parameters of $CD8^+$ T cell epitopes, we used the cancer testis antigen NY-ESO-1 (ESO) and HLA-A*0201 (A2). This non-mutated TA is expressed on a wide range of tumors, is highly immunogenic, has been used in diverse vaccine studies, and $CD8^+$ T cell responses have been studied extensively (22-27). Four A2-restricted ESO epitopes have been described, which are naturally produced and presented by APC, two of which are expressed by tumor cells (25,28-31). ESO-specific $CD8^+$ T cells responses in humans exhibit a strong immunodominance hierarchy and diverse HLA restrictions (32,33). Here we used different *in silico* servers to predict the binding strength, complex kinetic stability and immunogenicity of A2-restricted 8-11mer ESO peptides. The 41 peptides with the highest predicted binding affinity were tested for i) binding to A2 using a refolding, a peptide rebinding assay (34,35) and an A2 stabilization assay on T2 cells (36); ii) A2-peptide complex kinetic stability at 37°C (34,35,37); iii) peptide immunogenicity in A2/DR1 transgenic H-$2^{-/-}$ mice (36,38-40) and iv) recognition by $CD8^+$ T cells from ESO vaccinated melanoma patients (29-31). Our results define parameters of peptide immunogenicity and provide new cues on how to improve T cell epitope discovery.

RESULTS

ESO peptide binding to A2 - To predict the binding of ESO 8 to 11mer peptides to A2 we used the NetMHC 3.4 server (5,41-43). By setting an affinity threshold of 3000 nM, 41 peptides were obtained (Table 1). Nineteen of these were 10 or 11mers, which was unusual, because the majority of A2 bound peptides normally, are 9 mers (13). The immunodominant $ESO_{157-165}$ peptide had an IC_{50} of 1015 nM and would have been missed when using the recommended cut-off of 500 nM (28,29). We also performed predictions using the IEDB MHC I prediction server (44) and obtained the same results plus 17 additional peptides with predicted IC_{50} values of 918-2700 nM, none of which have been reported previously (Table S1).

Binding of the peptides to A2 was measured in a refolding assay (45). The most efficient refolding was observed for peptide 4, referred to as 100%, followed by peptides 6 (90%), 5 (87%), 31 (83%) and 1 (80%) (Figs. 1A,B). The correlation between measured and predicted peptide binding exhibited a Pearson coefficient of r = 0.64 and strong divergences for the peptides with high refolding scores (Fig. S1A). Similar correlations were observed when peptide binding was predicted with the more recent NetMHC 4.0 or NetMHCpan servers (9,12) (Figs. S1B,C). Comparable binding values were observed when using a peptide-rebinding assay (r = 0.97) (Figs. 1B,C). Repeating these experiments with different batches of peptides cautions that errors in the peptides (e.g. impurities and degradations) can be larger than those of these assays. We also assessed ESO peptide binding by an A2 complex stabilization on $A2^+$, TAP^- T2 cells (36) and obtained grossly different results, which may be explained by that A2 peptide stabilization on these cells relies on different mechanisms, the relative contributions of which are peptide dependent (data not shown) (46).

A2-ESO peptide complexes kinetic stability – The kinetic stability of the A2-ESO peptide complexes obtained in > 30% yields was assed at 37°C and their half-lives ($\tau_{1/2}$) calculated (Fig. 2A). Of the 20 complexes analyzed, the $\tau_{1/2}$ ranged between 1.82 h (peptide 29) and 13.5 h (peptide 1). The most stable complexes were those containing the peptides 1, 4, 16, 31 and the Flu $matrix_{58-66}$ peptide. These peptides also exhibited strong A2 binding (Fig. 1A); however other peptides exhibited robust A2

binding, but low kinetic complex stability and the overall correlation between measured A2 binding and complex kinetic stability was poor (r = 0.54) (Fig. 2B). The measured complexes stabilities correlated even less well with those predicted by the NetMHCstabpan (9) or the NetMHCstab server (47) (r = 0.31 and 0.47) (Fig. S1D,E). It noteworthy that the correlation between predicted complex stabilities and predicted binding affinities was better when using the NetMHC 3.4 rather than the more recent NetMHC 4.0 server (r = 0.58 and 0.33, respectively) (Figs. 2C,S1F).

ESO peptide's immunogenicity - To assess the ESO peptide's immunogenicity in mice, groups of A2/DR1 transgenic H-2$^{-/-}$ animals were immunized with pools of five peptides of comparable A2 binding affinity. Fourteen days after a booster immunization CD8$^+$ T cell splenocytes were isolated and tested for IFNγ production by ELISPOT upon incubation with single peptide pulsed T2 cells. For the ten peptides 1-4, 6, 8, 14, 16, 31 and 32 IFNγ responses were observed in the range of 30 - 108 spots per 10^5 T cells (Fig. 3A). The strongest responses were observed for the peptides 1, 4, 8, 16 and 32.

To assess the peptide's immunogenicity in humans, purified CD8$^+$ T cells from two melanoma patients vaccinated with recombinant vaccinia and fowl pox vectors expressing full-length ESO (23) were stimulated with the ESO peptides and assayed for IFNγ ELISPOT upon incubation with ESO peptide pulsed T2 cells. Strong IFNγ responses (600 - 800 spots per 10^5 T cells) were observed on the cells from patient NW 1789 for the peptides 1, 4, 6, 16 and 31 (Figs. 3B,S2A, blue bars). Lower responses were observed when autologous DC were used as APC (Figs. 3B, S2A, red bars). The peptide dependent variations of the reductions may be explained by biased peptide presentation by T2 cells; e.g. the peptides 6 and 31 had higher binding scores on T cells than the peptides 1, 4 and 16. It may also be that on DC some peptides are presented by HLA-alleles other than A2, which on T2 cells is unlikely, because these express A2 and only scant levels of HLA-B51 and Cw1 (Fig. S2B)(48). For the peptides 4, 16 and 31 CD8$^+$ T cell responses have been described previously (Fig. S3). The peptide $ESO_{155-163}$ was missed, because its predicted binding affinity was 3319 nM, i.e. above the cut-off of 3000 nM used. The A2-restriced CD8$^+$ T cell responses for the peptides 1 and 6 have not been reported previously. Remarkably, the ESO peptides 2, 3, 8 and 14 were immunogenic in A2 transgenic mice, but not in humans (Fig. 3).

Parameters defining the ESO peptide's immunogenicity – The peptides that were immunogenic in humans exhibited the highest A2 binding and kinetic complex stability (Fig. 2B). For the peptides immunogenic in mice only, both parameters were slightly lower. All immunogenic peptides exhibited complex stabilities of > 4h and refolding scores of >50% and all non-immunogenic peptides lower values. No such correlation was observed when peptide-binding affinity was predicted using the NetMHC 3.4 (6,42), NetMHC 4.0 (12) or NetMHCpan (9) server or kinetic A2-ESO peptide complex stability using the NetMHCstab (47) or NetMHCstabpan (16) server (Figs. 2C,S1). However, for most of the ESO peptides the T cell epitope scores predicted by the NetTepi server (20) correlated better with the measured binding strength and kinetic complex stability, respectively (Figs. 4A,B). The three outliers included the therapeutically important peptide 31.

Of the ten ESO immunogenic peptides, five (1, 4, 6, 16 and 31) contained the $ESO_{159-165}$ sequence (LMWITQC) and were immunogenic in humans and A2 transgenic mice (Fig. 4C,E). The peptides 2, 8, 14 and 32 were immunogenic only in mice and contained the sequence $ESO_{110-116}$ (AQDAPPL). Only the sequence of the ESO_{86-94} peptide was outside these two registers (Figs. 3,4C,E). When bound to A2, generally the side chains of the second and the last (C-terminal) residues occupy the B and F pockets, while the side chains of the others are solvent exposed to different degrees and some can be secondary anchor residues (49-51). The peptides comprising the $ESO_{159-165}$ core sequence exhibited 4-5 large aliphatic and/or aromatic residues in these positions, whereas the peptides containing the $ESO_{110-116}$ core sequence only one or none (Fig. 4D). Two studies have shown that immunogenic peptides express such amino acids in solvent exposed positions (18,19). Indeed, the immunogenicity scores calculated with the IEDB immunogenicity predictor (http://tools.iedb.org/immunogenicity/), which takes TCR propensity into account, were higher for the peptides containing the $ESO_{159-165}$ core sequence (0.17 - 0.25) than those containing the $ESO_{110-116}$ sequence (-0.06 - 0.009) (Table 1).

The correlations between predicted and measured peptide binding and kinetic pMHC complex stability in our study were poorer compared to those reported in other studies (Figs. S1A-E)(9,16,42,43). In these studies and for the training of the prediction servers, pathogen-derived antigens were used. To address the question whether there are differences between TA and pathogen-derived peptides, we examined 149 non-mutated TA and 129

viral T cell epitopes. All peptides were A2-restricted nonamers and collected from databases (Table S2). Positional amino acid usage of these peptides was analyzed with the Seq2Logo server (52). This revealed that in the main A2 anchor positions 2 and 9 L was more frequent in TA peptides, especially in P9, in which V was the most abundant residue in viral peptides (Figs. S4A,B). Moreover, viral peptides exhibited higher amino acid diversity especially in positions 3 and 7, which typically are secondary A2 anchor residues (50,51). We next calculated the average hydrophobicity scores for the residues in positions 1-9 for the two sets of peptides using the scales published by Kyte and Doolittle (53). The hydrophobicity was highest for the residues in position 2 and 9 and lowest for those in position 4 (Fig. S4C). Similar results were obtained when other amino acid hydrophobicity scales were used, i.e. those determined by Hopp & Woods, Abraham & Leo, Black & Mould, Sweet & Eisenberg and Roseman, as detailed in http://web.expasy.org/protscale/ (Fig. S4D). The TA peptides exhibited higher hydrophobicity in all positions, except for position 3. In position 4 viral but not TA peptide frequently contained acidic residues, resulting in greatly reduced average hydrophobicity. As illustrated in structure of the A2-HIV $RT_{309-317}$ complex, an acidic residue in position 4 can stably bind to the A2 α1 helix (R65)(51). Moreover, viral peptides contained more polar and/or charged residues in positions 1 and 7 than TA peptides, accounting for their overall modestly reduced hydrophobicity. Collectively these results argue that at large there exist differences between TA and viral peptides, notably in amino acid usages in A2 anchor positions.

DISCUSSION

A widely used strategy to identify T cell epitopes consists in first predicting HLA binding peptides by *in silico* algorithms (13,34,35,54). Here we predicted A2-restricted 8-11mer peptides of ESO using the NetMHC 3.4 and IEDB servers and obtained partially overlapping results, which was explained by that these servers are based on related ANN (Tables 1 and S1) (6,41,42,44). Testing of the 41 peptides with the highest predicted binding affinity gave very similar results when using the refolding or peptide rebinding assay (Fig. 1).

There exist diverse *in silico* MHC-peptide binding predictors of which the ANN based NetMHC servers performed best in benchmark studies (8,43,55). We examined correlations between measured A2 ESO peptide binding and NetMHC 3.4 and the more recent NetMHC 4.0 or NetMHCpan 3.0 servers that allow insertions and deletions in peptide alignments and integration of multiple receptor and peptide length data sets, respectively (6,9,12,42). Surprisingly these refinements did not improve the correlations between measured and predicted ESO-peptide binding (Figs. S1A-C). Poorer correlations were observed when peptide binding was predicted with the PickPocket, SYFPEITHI or Rankpeptide servers, which is consistent with other reports (unpublished results)(8,11,43,55). One explanation for the modest correlation between measured and predicted ESO peptide binding could be that the predicted binding affinities represent IC_{50} values in nM, whereas in our study relative binding values were measured at a fixed peptide concentration. However, in our system the measured IC_{50} values correlated even less well with NetMHC 3.4 predicted values ($r = 0.56$, $p < 0.0001$)(unpublished results).

We next measured the A2-ESO complex stabilities and found that the measured values poorly correlated with those predicted by the NetMHCstab and the more recent NetMHCstabpan server (Figs. S1D,E) (16,47). The measured ESO peptide binding and kinetic complex stability exhibited a modest correlation (Fig. 2B), which is consistent with the fact that peptide binding and kinetic pMHC complex stability can diverge; it has been shown that for complex stability, but much less for peptide binding affinity, fitting of the side chains of the residues in position 2 and 3 into HLA binding pockets is critical (37,47,56). In this plot all immunogenic peptides exhibited complex stabilities of >4h and peptide binding efficiencies of >50% (Figs. 2B,3, Table 1). The highest peptide binding strengths and complex stabilities were observed for the ESO peptides immunogenic in humans, followed by those immunogenic in A2 transgenic mice only. Our results are in accordance with an analysis of large data sets showing that immunogenic peptides typically exhibit high binding affinity and high complex kinetic stability (57), but are at variance with studies reporting that peptide immunogenicity correlates with binding affinity (5,34,58) and pMHC complex kinetic stability (16,34,37), respectively. No significant correlation was observed between peptide immunogenicity, binding strength and complex kinetic stability when complex stability was predicted by the NetMHCstabpan and binding affinity by the NetMHC 3.4 or NetMHC 4.0 server (Figs. 2C,3,S1F). There was also no correlation between peptide's immunogenicity and predicted binding affinity and kinetic complex stability,

respectively (Figs. 3,S1A-E, Table 1). Moreover, our results caution that selection of peptides based *in silico* predictions using a cut-off affinity of 500 nM is prone to miss immunogenic peptides; in our study three peptides, including the clinically important peptide 31 (Fig. S3, Table 1). The same is true for other clinically important TA epitopes like the A2-restricted Melan-A_{26-35} (EAAGIGILTV) (5164 nM), survivin$_{96-104}$ (LTLGEFLKL) (2002 nM) or $CEA_{694-702}$ (GVLVGVALI) (833 nM) peptides (http://www.iedb.org). It is important to note that CTL tumor control depends more on the affinity of pMHC-TCR than on MHC-peptide binding (59).

The correlations between measured and predicted peptide binding strength and kinetic complex stability were poorer in our study compared to those in other studies (Fig. S1A-E)(9,16,42,43). In these and for training of the prediction servers pathogen derived antigens were mainly used. Tumor antigens excluding neoantigens are *a priori* self-antigens and hence are subject to central tolerance, which is not the case for pathogen-derived antigens (60,61). By comparing 149 TA and 129 viral A2 restricted nona-peptides, we observed significant differences in amino acid usages and average hydrophobicity in the potential secondary anchor residues in positions 1, 4 and 7 and smaller ones in the potential main A2 anchor residues in positions 2 and 9 (Fig. S4, Table S2). It has been demonstrated that changes in HLA-peptide anchoring can alter the conformation and flexibility of pMHC complexes and thus their interaction with TCR (62-65). The significance of such changes is illustrated e.g. by modification of a potential main anchor residue (A27L) in the Melan-A_{26-25} peptide, which resulted in different TCR interactions and different outcomes of vaccine trials (64,65). Thus the limited *in silico* prediction accuracy of TA peptides may be explained by that the servers were trained on pathogen-derived peptides. It is noteworthy that a substantial fraction of neoepitopes contains a mutation in an MHC anchor position, some of which may affect T cell recognition via structural changes in the pMHC complex and binding to TCR (1,2,15,58,62,63). It should be mentioned that most neoepitopes contain a stochastic somatic mutation, which can have different and diverse effects, making general predictions difficult.

An unexpected finding was that immunization of A2 transgenic mice induced CTL for ten of the ESO peptides, whereas in humans T cells specific for only five were observed (Figs. 3,S2,S3). This observation cautions that peptides can be immunogenic in HLA transgenic mice but not in humans. All ESO peptides that were immunogenic in humans contained the sequence $ESO_{159-165}$ (LMWITQC) (Figs. 3,4C-E). When bound to A2 these peptides contained amino acids with potentially solvent exposed large hydrophobic and/or aromatic side chains, which have been shown to convey immunogenicity (18,19). Conversely, the peptides 2, 8, 14, and 32 that were immunogenic only in A2 transgenic mice, contained the $ESO_{110-116}$ sequence (AQDAPPL). When bound to A2, these peptides contained one or no such residue (Figs. 4C-E). In accordance with this, the immunogenicity scores predicted by the IEDB immunogenicity server, which considers peptide's TCR propensity, were substantially lower for these than the former peptides (Table 1)(18).

However, peptide 3 contained several hydrophobic/aromatic residues, had high immunogenicity scores, yet was not immunogenic in humans and only weakly in A2 transgenic mice, arguing that immunogenicity also depends on other factors, such as: i) in humans, but not in HLA transgenic H-$2^{-/-}$ mice, ESO peptides can be presented and recognized in the context of other HLA alleles; e.g. HLA-B35 and Cw3 for which immunodominant ESO CTL responses are known (27,32,33); ii) the efficiency of peptide production and presentation by APC. *In silico* predictions and *in vitro* digestion experiments argue that human proteasomes produce the peptides that were immunogenic in mice, but not in humans (Fig. 4E) (14,32,66). Indeed, CTL were found in cancer patients with such specificities but other HLA restrictions (32,33,67). iii) Peptides binding to multiple HLA alleles, including HLA class II molecules are more immunogenic than those binding to only one allele (32,40,68). For the $ESO_{159-165}$ core sequence-containing peptides there is the strongly immunogenic, DP4-restricted T cell epitope $ESO_{157-170}$ (69), whereas for the $ESO_{110-116}$ core sequence containing peptides no $CD4^+$ T cell epitope is known. iv) Non-mutated TA, including ESO, are self-antigens and therefore TA-specific T cell responses are pruned by central tolerance in humans, which is not the case in mice that lack ESO (22,60,61).

In conclusion, our study demonstrated that only a small fraction of A2 binding ESO peptides was immunogenic in humans, namely those that had high peptide binding strength and kinetic complex stability. These peptides contained multiple hydrophobic/aromatic residues, supporting the notion that immunogenicity correlates with TCR propensity. There is a need to improve *in silico* predictions of peptide's binding properties and immunogenicity of TA, namely by considering structural/conformational

aspects of MHC-peptide binding, training of prediction servers with TA peptides and refining TCR propensity calculations.

EXPERIMENTAL PROCEDURES

Peptides - Peptides were produced by the Protein and Peptide Chemistry Facility (PPCF) of the University of Lausanne, were HPLC purified (>95 % pure), verified by mass spectrometry and kept lyophilized at -80°C.

In silico prediction of HLA-A0201 epitopes from NY-ESO-1 - To predict A2 restricted ESO 8-11mer peptides, we used the NetMHC-3.4 server (6,42) and selected the 41 peptides scoring with an IC_{50} <3000 nM; they were additionally submitted to the NetMHC 4.0 (12) and the NetMHCpan servers (9) for binding affinity predictions and the NetMHCstab (47) and the NetMHCstabpan (16) servers for A2-ESO complex kinetic stability predictions, respectively. For immunogenicity predictions, the NetTepi server (20) and the IEDB MHC I immunogenicity servers (http://tools.iedb.org/immunogenicity/) were used.

Peptide-driven refolding assay - Refolding with A2 heavy chain carrying a C-terminal BirA substrate peptide (BSP), Cy5-labeled β2m and a test peptide were performed essentially as described (45). Human β2m was mutated S88 to C and after refolding alkylated with maleimide-PEG_2-Cy5 (Pierce, Thermo Fisher Scientific) in PBS at pH 7.4. Refolding reactions were performed in 96 well plates at 4°C for 72 h in the presence of 10 µM peptide. Incubation without peptide and with the Flu $matrix_{58-66}$ peptide served as negative and positive controls, respectively. After centrifugation (4'000 rpm, 5 min), the reaction mixtures were transferred into 96 well plates and Cy5 fluorescence read on a fluorescence plate reader (Modulus, Promega). All measurements were performed in triplicates and data processed using Excel (Microsoft).

Peptide rebinding and pMHC complex kinetic stability assays - Ninety-six well plates were coated with streptavidin and biotinylated A2-$MelanA_{26-35}$ complexes (1 µg/ml) were added in 50 µl and incubated for 2 h at 4°C. The plates were saturated with biotin, washed and incubated for 3 min at 4°C with citrate buffer (citric acid 0.13 M, Na_2HPO_4 66 mM, NaCl 150 mM; pH 4.0), followed by washing with PBS containing 0.05 % Tween 20. Test peptides (10 µM) and Cy5-labeled β2m were added in PBS containing 5 mM EDTA and the plates incubated at 4°C for 72 h. After washing with PBS containing 0.05 % Tween 20, the A2-peptide complexes were quantified as described above. Incubations without peptide and with the Flu $matrix_{58-66}$ peptide served as negative and positive controls, respectively. The kinetic stability of complexes was assessed by incubating the A2-peptide complexes at 37°C and after different period of times their content was quantified likewise. Results were plotted and half-lives determined using GrapPad Prism software (GraphPad, San Diego, USA). All measurements were performed in triplicates.

Immunization of A2 transgenic mice - HLA-A2/DR1 transgenic, $H\text{-}2^{-/-}$ mice (38) were obtained from Taconic (https://www.taconic.com) and maintained in the Institute's animal facility and used in accordance with the Cantonal Veterinary Office. Groups of mice (n = 5) were immunized with peptides essentially as described (39). In brief, pools of five ESO peptides of similar affinities for A2 and the DR1 restricted influenza $HA_{306-318}$ peptide (10 µg each) were injected sc. at the base of the tail in an emulsion containing PBS, IFA and ODN 1826 (InvivoGen, San Diego). After two weeks mice were booster immunized and a fortnight later their spleens harvested, the $CD8^+$ T cells purified by negative selection (Stemcell Technologies, Köln, Germany) and incubated overnight with T2 cells previously pulsed with 1 µM of peptide at a 1:1 ratio. Production of IFNγ was assessed using a mouse ELISPOT kit following the manufacturer's instructions (Mabtech, Nacka Strand, Sweden).

Analysis of NY-ESO-1-specific CTL from patient - Isolation, culturing and stimulation of PBMC and $CD8^+$ T cells from melanoma patient NW1789 and NW3276 followed established procedures (31). In brief, purified $CD8^+$ T cells were stimulated twice with 1 µM of ESO peptides, irradiated autologous PBMC and 150 U/ml of IL2. After a fortnight the CTL were tested for IFNγ production by ELISPOT following incubation with ESO peptide-pulsed T2 cells or autologous DC. A positive response was considered if the number of spots in the peptide-exposed well was > 2-fold higher than the number of spots in the un-stimulated well, and there were > 10 specific spots/25,000 T cells. The generation of DC and the ELISPOT assay were performed as described (31).

Statistics - Statistical analyses were performed using the GraphPad Prism software (GraphPad, San Diego, USA). Correlation analyses were performed using Pearson coefficient r. The associated p value (two-tailed, $\alpha = 0.05$) quantifies the likelihood that the correlation is due to random sampling.

Acknowledgments: This work was supported by Swiss National Science Foundation grant 310030_12533/1. We gratefully acknowledge helpful discussions with Drs D. Gfeller, M. Bassani-Sternberg and A. Harari, R. Genolet and D. Kouzentsov for invaluable help in data processing, presentation and computing.

Conflict of interest: The authors declare no conflicts of interest.

Author contributions: J.S. and P.G. performed the biochemical assays, which were established and optimized by D.D.; J.K. performed all the experiments on human cells; J.S. performed *in silico* predictions, data processing and statistical analysis; I.L. and C.C. coordinated the study and edited the manuscript and all authors discussed and interpreted results.

REFERENCES

1. Schumacher, T.N., and Hacohen, N. (2016) Neoantigens encoded in the cancer genome. *Curr. Opin. Immunol*. 2016;**41**:98-103.
2. Schumacher, T.N., and Schreiber, R.D. (2015) Neoantigens in cancer immunotherapy. *Science.* **348**(6230):69-74.
3. Bassani-Sternberg, M., and Coukos, G. (2016). Mass spectrometry-based antigen discovery for cancer immunotherapy. *Curr Opin Immunol*. **41**:9-17.
4. Bassani-Sternberg, M., Bräunlein ,E., Klar, R., Engleitner, T., Sinitcyn, P., Audehm, S., Straub, M., Weber, J, Slotta-Huspenina, J, Spech,t K, Martignoni, ME, Werner, A, Hein, R, H Busch, D, Peschel, C, Rad, R, Cox, J, Mann, M, and Krackhardt, AM. (2016) Direct identification of clinically relevant neoepitopes presented on native human melanoma tissue by mass spectrometry. *Nat Commun*. **7**:13404.
5. Lund, O., Nascimento, E.J, Maciel, M Jr, Nielsen, M., Larsen, M.V., Lundegaard, C., Harndahl, M., Lamberth, K., Buus, S., Salmon, J., August, T.J., and Marques, E.T. Jr. (2011) Human leukocyte antigen (HLA) class I restricted epitope discovery in yellow fewer and dengue viruses: importance of HLA binding strength. *PLoS One*. **6**(10):e26494.
6. Lundegaard, C., Lund, O., and Nielsen, M. (2008) Accurate approximation method for prediction of class I MHC affinities for peptides of length 8, 10 and 11 using prediction tools trained on 9mers. *Bioinformatics*. **24**(11):1397-8.
7. Vita, R., Zarebski, L., Greenbaum, J.A., Emami, H., Hoof, I., Salimi, N., Damle, R., Sette, A., and Peters, B. (2010) The immune epitope database 2.0. *Nucleic Acids Res*. **38**:D854-62.
8. Backert, L., and Kohlbacher O. (2015). Immunoinformatics and epitope prediction in the age of genomic medicine. *Genome Med*.**7**:119.
9. Nielsen, M., Andreatta, M. (2016) NetMHCpan-3.0; improved prediction of binding to MHC class I molecules integrating information from multiple receptor and peptide length datasets. *Genome Med*.**8**(1):33.
10. Carrasco, Pro, S, Zimic, M, and Nielsen, M. (2014) Improved pan-specific MHC class I peptide-binding predictions using a novel representation of the MHC-binding cleft environment. *Tissue Antigens*. **83**(2):94-100.
11. Zhang H., Lund O., and Nielsen, M. (2009) The PickPocket method for predicting binding specificities for receptors based on receptor pocket similarities: application to MHC-peptide binding. *Bioinformatics*. **25**(10):1293-9.
12. Andreatta, M., and Nielsen, M. (2016). Gapped sequence alignment using artificial neural networks: application to the MHC class I system. *Bioinformatics* **32**(4):511-7.
13. Trolle,T., McMurtrey, C.P, Sidney, J., Bardet, W., Osborn, S.C., Kaever, T., Sette, A., Hildebrand, W.H., Nielsen, M., and Peters., B. (2016) The Length Distribution of Class I-Restricted T Cell Epitopes Is Determined by Both Peptide Supply and MHC Allele-Specific Binding Preference. *J Immunol*. **196**(4):1480-7.
14. Calis, J.J., Reinink, P., Keller, C., Kloetzel, P.M., and Keşmir, C. (2015) Role of peptide processing

predictions in T cell epitope identification: contribution of different prediction programs. *Immunogenetics*. **67**(2):85-93.
15. van Buuren, M.M., Calis, J.J., and Schumacher, T.N. (2014) High sensitivity of cancer exome-based CD8 T cell neo-antigen identification. *Oncoimmunology*. **3**:e28836.
16. Rasmussen, M., Fenoy, E., Harndahl, M., Kristensen, A.B., Nielsen, I.K., Nielsen, M., and Buus, S. (2016). Pan-Specific Prediction of Peptide-MHC Class I Complex Stability, a Correlate of T Cell Immunogenicity. *J Immunol*. 5;**197**(4):1517-24.
17. Wu, X., Xu, X., Gu, R., Wang, Z., Chen, H., Xu K., Zhang, M., Hutton, J., and Yang, T. (2012) Prediction of HLA class I-restricted T-cell epitopes of islet autoantigen combined with binding and dissociation assays. *Autoimmunity*. **45**(2):176-85.
18. Calis, J.J., Maybeno, M., Greenbaum, J.A., Weiskopf, D., De Silva, A.D., Sette, A., Keşmir, C., and Peters, B. (2013). Properties of MHC class I presented peptides that enhance immunogenicity. *PLoS Comput Biol*. **9**(10):e1003266.
19. Chowell, D., Krishna, S., Becker, P.D., Cocita, C., Shu, J., Tan, X., Greenberg, P.D., Klavinskis, L.S., Blattman, J.N., and Anderson, K.S. (2015) TCR contact residue hydrophobicity is a hallmark of immunogenic CD8+ T cell epitopes. *Proc Natl Acad Sci U S A*.**112**(14):E1754-62.
20. Trolle T., and Nielsen, M. (2014) NetTepi: an integrated method for the prediction of T cell epitopes. *Immunogenetics.* **66**(7-8):449-56.
21. Gilchuk, P., Hill, T.M., Wilson, J.T., and Joyce, S. (2015) Discovering protective CD8 T cell epitopes--no single immunologic property predicts it! *Curr Opin Immunol*. **34**:43-51.
22. Esfandiary, A, and Ghafouri-Fard, S. New York esophageal squamous cell carcinoma-1 and cancer immunotherapy. *Immunotherapy*.**7**(4):411-39.
23. Odunsi, K., Matsuzaki, J., Karbach, J., Neumann, A., Mhawech-Fauceglia, P., Miller, A., Beck, A., Morrison, C.D., Ritter, G., Godoy, H., Lele, S., DuPont, N., Edwards, R., Shrikant, P., Old, L.,J., Gnjatic, S., and Jäger, E.. (2012) Efficacy of vaccination with recombinant vaccinia and fowlpox vectors expressing NY-ESO-1 antigen in ovarian cancer and melanoma patients. *Proc Natl Acad Sci U S A*. **109**(15):5797-802.
24. Valmori, D., Dutoit, V., Liénard, D., Rimoldi, D., Pittet, M.J., Champagne, P., Ellefsen, K., Sahin, U., Speiser, D., Lejeune, F., Cerottini, JC, and Romero, P. (2000). Naturally occurring human lymphocyte antigen-A2 restricted CD8+ T-cell response to the cancer testis antigen NY-ESO-1 in melanoma patients. C*ancer Res*. **60**(16):4499-506.
25. Gnjatic, S., Jäger, E., Chen, W., Altorki, N.K., Matsuo, M., Lee, S.Y., Chen, Q., Nagata, Y., Atanackovic, D., Chen, Y.T., Ritter, G., Cebon, J., Knuth, A., and Old, L.J. (2002) CD8(+) T cell responses against a dominant cryptic HLA-A2 epitope after NY-ESO-1 peptid immunization of cancer patients. *Proc Natl Acad Sci U S A*. **99**(18):11813-8.
26. Bioley, G., Guillaume, P., Luescher, I., Bhardwaj, N., Mears, G., Old L., Valmori, D., and Ayyoub, M. (2009) Vaccination with a recombinant protein encoding the tumor-specific antigen NY-ESO-1 elicits an A2/157-165-specific CTL repertoire structurally distinct and of reduced tumor reactivity than that elicited by spontaneous immune responses to NY-ESO-1-expressing Tumors. *J Immunother*. **32**(2):161-8.
27. Bioley, G., Guillaume, P., Luescher, I., Yeh, A., Dupont, B., Bhardwaj, N., Mears, G., Old, L.J., Valmori, D., and Ayyoub, M. (2009) HLA class I - associated immunodominance affects CTL responsiveness to an ESO recombinant protein tumor antigen vaccine. *Clin Cancer Res*. **15**(1):299-306.
28. Dutoit, V., Taub, R.N., Papadopoulos, K.P., Talbot, S., Keohan, M.L., Brehm, M., Gnjatic, S., Harris, P.E., Bisikirska, B., Guillaume, P., Cerottini, J.C., Hesdorffer, C.S., Old, L.J., and Valmori, D. (2002) Multiepitope CD8(+) T cell response to a NY-ESO-1 peptide vaccine results in imprecise tumor targeting. *J Clin Invest*. **110**(12):1813-22.
29. Jäger, E., Chen, Y.T., Drijfhout, J.W., Karbach, J., Ringhoffer, M., Jäger, D., Arand, M., Wada, H., Noguchi, Y., Stockert, E., Old, L.J., and Knuth, A. (1998) Simultaneous humoral and cellular immune response against cancer-testis antigen NY-ESO-1: definition of huma histocompatibility leukocyte antigen (HLA)-A2-binding peptide epitopes. *J Exp. Med*. **187**(2):265-70.
30. Jäger, E., Karbach, J., Gnjatic, S., Neumann, A. Bender, A., Valmori, D., Ayyoub, M., Ritter, E., Ritter, G., Jäger, D., Panicali, D., Hoffman, E., Pan, L., Oettgen, H., Old, L.J., and Knuth, A. (2006) Recombinant vaccinia/fowlpox NY-ESO-1 vaccines induce both humoral and cellular NY-ESO-1-

specific immune responses in cancer patients. *Proc Natl Acad Sci U S A.*;**103**(39):14453-8.
31. Karbach, J., Gnjatic, S., Pauligk, C., Bender, A., Maeurer, M., Schultze, J.L., Nadler, K., Wahle, C., Knuth, A., Old, L.J., and Jäger, E. (2007) Tumor-reactive CD8+ T-cell clones in patients after NY-ESO-1 peptide vaccination. *Int J Cancer*. **121**(9):2042-8.
32. Valmori, D., Lévy, F., Godefroy, E. Scotto, L., Souleimanian, N.E., Karbach, J., Tosello, V., Hesdorffer, C.S., Old, L.J., Jager, E, and Ayyoub, M. (2007) Epitope clustering in regions undergoing efficient proteasomal processing defines immunodominant CTL regions of a tumor antigen. *Clin Immunol*. **122**(2):163-72.
33. Jackson, H., Dimopoulos, N., Mifsud, N.A., Tai, T.Y., Chen, Q., Svobodova, S., Browning, J., Luescher I., Stockert, L., Old, L.J., Davis, I.D., Cebon, J., and Chen, W. (2006) Striking immunodominance hierarchy of naturally occurring CD8+ and CD4+ T cell responses to tumor antigen NY-ESO-1. *J Immunol*.**176**(10):5908-17.
34. Fridman, A., Finnefrock, A.C., Peruzzi, D., Pak, I., La Monica, N., Bagchi, A., Casimiro, D.R., Ciliberto, G., and Aurisicchio, L. (2012) An efficient T-cell epitope discovery strategy using in silico prediction and the iTopia assay platform. *Oncoimmunology.***1**(8):1258-1270.
35. Axelsson-Robertson, R., Weichold, F., Sizemore, D., Wulf, M, Skeiky, Y.A., Sadoff, J., and Maeurer, M.J. (2010) Extensive major histocompatibility complex class I binding promiscuity for Mycobacterium tuberculosis TB10.4 peptides and immune dominance of human leucocyte antigen (HLA)-B*0702 and HLA-B*0801 alleles in TB10.4 CD8 T-cell responses. *Immunology*. **129**(4):496-505.
36. Duan, Z.L., Li, Q., Wang, Z.B., Xia, K.D., Guo, J.L., Liu, W.Q., and Wen, J.S. (2012) HLA-A*0201-restricted CD8+ T-cell epitopes identified in dengue viruses. *Virol J.* **9**:259.
37. Harndahl, M., Rasmussen M., Roder G., Dalgaard Pedersen I., Sørensen, M, Nielsen M., and Buus, S. (2012) Peptide-MHC class I stability is a better predictor than peptide affinity of CTL immunogenicity. *Eur J Immunol*. **42**(6):1405-16.
38. Pajot, A., Michel, M.L., Fazilleau, N., Pancré, V., Auriault, C., Ojcius, D.M., Lemonnier, F.A., and Lone, Y.C. (2004) A mouse model of human adaptive immune functions in HLA-A2.1-/HLA-DR1-transgenic H-2 class I-/class II-knockout mice. *Eur J Immunol*. **34**(11):3060-9.
39. Boucherma, R., Kridane-Miledi H., Bouziat R,. Rasmussen M., Gatard T., Langa-Vives, F., Lemercier, B., Lim, A., Bérard, M., Benmohamed, L., Buus, S., Rooke, R., and Lemonnier, F.A. (2013) HLA-A*01:03, HLA-A*24:02, HLA-B*08:01, HLA-B*27:05, HLA-B*35:01, HLA-B*44:02, and HLA-C*07:01 monochain transgenic/H-2 class I null mice: novel versatile preclinical models of human T cell responses. *J Immunol*. **191**(2):583-93.
40. Nascimento, E.J., Mailliard, R.B, Khan, A.M., Sidney, J., Sette, A., Guzman, N., Paulaitis, M., de Melo, A.B., Cordeiro, M.T., Gil, L.V., Lemonnier, F., Rinaldo, C., August, J.T., and Marques, E.T. Jr. (2013) Identification of conserved and HLA promiscuous DENV3 T-cell epitopes. *PLoS Negl Trop Dis*.**7**(10):e2497.
41. Lundegaard, C., Lund, O., and Nielsen, M. (2011) Prediction of epitopes using neural network based methods. *J Immunol Methods*.**374**(1-2):26-34.
42. Lundegaard, C., Lamberth, K., Harndahl, M., Buus, S., Lund, O., and Nielsen, M. (2008) NetMHC-3.0: accurate web accessible predictions of human, mouse and monkey MHC class I affinities for peptides of length 8-11. *Nucleic Acids Res*.**3**:W509-12.
43. Trolle, T., Metushi, I.G., Greenbaum, J.A., Kim, Y., Sidney, J., Lund, O,. Sette, A., Peters, B., and Nielsen, M. (2015) Automated benchmarking of peptide-MHC class I binding predictions. *Bioinformatics*. **31**(13):2174-81.
44. Kim, Y, Ponomarenko, J, Zhu Z, Tamang, D, Wang, P, Greenbaum, J, Lundegaard, C, Sette, A, Lund, O, Bourne, PE, Nielsen, M, and Peters, B. (2012) Immune epitope database analysis resource. *Nucleic Acids Res*. **40**W525-30.
45. Guillaume, P., Legler, D.F., Boucheron, N., Doucey, M.A., Cerottini, J.C., and Luescher, I.F. (2003) Soluble major histocompatibility complex-peptide octamers with impaired CD8 binding selectively induce Fas-dependent apoptosis. *J Biol Chem*. **278**(7):4500-9.
46. Luft, T., Rizkalla, M., Tai, T.Y., Chen, Q., MacFarlan, R.I., Davis, I.D., Maraskovsky, E., and Cebon, J. (2001) Exogenous peptides presented by transporter associated with antigen processing (TAP)-deficient and TAP-competent cells: intracellular loading and kinetics of presentation. *J Immunol*. **167**(5):2529-37.

47. Jørgensen, K.W., Rasmussen, M., Buus, S, and Nielsen, M. (2014) NetMHCstab -predicting stability of peptide-MHC-I complexes; impacts for cytotoxic T lymphocyte epitope discovery. *Immunology*. **141**(1):18-26.
48. Salter, R.D., and Cresswell, P. (1986) Impaired assembly and transport of HLA-A and –B antigens in a mutant TxB cell hybrid. *EMBO J*. **5**(5):943-9.
49. Chen, J.L., Stewart-Jones, G., Bossi, G., Lissin, N.M., Wooldridge, L., Choi, E.M., Held, G., Dunbar, P.R., Esnouf, R.M., Sami, M., Boulter, J.M., Rizkallah, P., Renner, C., Sewell, A, van der Merwe, P.A., Jakobsen, B.K., Griffiths, G., Jones, E.Y., Cerundolo, V. (2005) Structural and kinetic basis for heightened immunogenicity of T cell vaccines. *J Exp Med*. **201**:1243-55.
50. Ruppert, J., Sidney, J., Celis, E., Kubo, R.T., Grey, H.M., and Sette, A. (1993) Prominent role of secondary anchor residues in peptide binding to HLA-A2.1 molecules. *Cell.* **74**(5):929-37.
51. Madden, D.R., Garboczi, D.N., and Wiley, D.C. (1993) The antigenic identity of peptide-MHC complexes: a comparison of the conformations of five viral peptides presented by HLA-A2. *Cell*. **75**(4):693-708.
52. Thomsen, M.C., and Nielsen, M. (2012) Seq2Logo: a method for construction and visualization of amino acid binding motifs and sequence profiles including sequence weighting, pseudo counts and two-sided representation of amino acid enrichment and depletion. *Nucleic Acids Res*. **40**, W281-7.
53. Kyte, J., and Doolittle, R.F. (1982) A simple method for displaying the hydropathic character of a protein. *J Mol Biol*. **157**(1):105-32.
54. Harndahl, M., Justesen, S., Lamberth, K., Røder, G., Nielsen, M., and Buus, S. (2009) Peptide binding to HLA class I molecules: homogenous, high-throughput screening, an affinity assays. *J Biomol Screen*. **14**(2):173-80.
55. Snyder, A., and Chan, T.A. (2015) Immunogenic peptide discovery in cancer genomes. *Curr Opin Genet Dev*. **30**:7-16.
56. Miles, K.M., Miles, J.J., Madura, F., Sewell, A.K, and Cole, D.K. (2011) Real time detection of peptide-MHC dissociation reveals that improvement of primary MHC-binding residues can have a minimal, or no, effect on stability. *Mol Immunol*. **48**(4):728-32.
57. Wang, S., Li, J., Chen, X., Wang, L., Liu, W., and Wu, Y. (2016) Analyzing the effect of peptide-HLA-binding ability on the immunogenicity of potential CD8+ and CD4+ T cell epitopes in a large dataset. *Immunol Res*. **64**(4):908-18.
58. Fritsch, E.F., Rajasagi, M., Ott, P.A., Brusic, V., Hacohen, N., and Wu, C.J. (2014) HLA-binding properties of tumor neoepitopes in humans. *Cancer Immunol Res*. **2**(6):522-9.
59. McMahan, R.H., McWilliams, J.A., Jordan, K.R., Dow, S.W., Wilson, D.B., and Slansky, J.E. (2006) Relating TCR-peptide-MHC affinity to immunogenicity for the design of tumor vaccines. *J Clin Invest*. **116**(9):2543-51.
60. Anderson, M.S., and Su, M.A. (2016) AIRE expands: new roles in immune tolerance and beyond. *Nat Rev Immunol*. **16**(4):247-58.
61. Khan, I.S., Mouchess, M.L., Zhu, M.L., Conley, B., Fasano, K.J., Hou, Y., Fong, L., Su, M.A., and Anderson, M.S. (2014) Enhancement of an anti-tumor immune response by transient blockade of central T cell tolerance. *J Exp Med*. **211**(5):761-8.
62. Duan, F., Duitama, J., Al Seesi, S., Ayres, C.M., Corcelli, S.A., Pawashe, A.P., Blanchard, T., McMahon, D., Sidney, J., Sette, A., Baker, B.M., Mandoiu, I.I., and Srivastava, P.K. (2014) Genomic and bioinformatic profiling of mutational neoepitopes reveals new rules to predict anticancer immunogenicity. *J Exp Med*. **211**(11):2231-48.
63. Hawse, W.F., Gloor, B.E., Ayres, C.M., Kho, K., Nuter, E., and Baker, B.M. (2013) Peptide modulation of class I major histocompatibility complex protein molecular flexibility and the implications for immune recognition. *J Biol Chem*. **288**(34):24372-81.
64. Madura, F., Rizkallah, P.J., Holland, C.J., Fuller, A., Bulek, A., Godkin, A.J, Schauenburg, A.J., Cole, D.K., and Sewell, A.K. (2015) Structural basis for ineffective T-cell responses to MHC anchor residue-improved "heteroclitic" peptides. *Eur J Immunol*. **45**(2):584-91
65. Insaidoo, F.K., Borbulevych, O.Y., Hossain, M., Santhanagopolan, S.M., Baxter, T.K., and Baker, B.M. (2011) Loss of T cell antigen recognition arising from changes in peptide and major histocompatibility complex protein flexibility: implications for vaccine design. *J Biol Chem*. **286**(46):40163-73.
66. Nielsen, M., Lundegaard, C., Lund, O., and Keşmir, C. (2005) The role of the proteasome in

generating cytotoxic T-cell epitopes: insights obtained from improved prediction of proteasomal cleavage. *Immunogenetics*. **57**(1-2):33-41.
67. Chen, J.L., Dawoodji, A., Tarlton, A., Gnjatic, S., Tajar, A., Karydis, I., Browning, J., Pratap, S., Verfaille, C., Venhaus, R.R., Pan, L., Altman, D.G., Cebon, J.S., Old, L.L., Nathan, P., Ottensmeier, C., Middleton, M., and Cerundolo, V. (2015) NY-ESO-1 specific antibody and cellular responses in melanoma patients primed with NY-ESO-1 protein in ISCOMATRIX an boosted with recombinant NY-ESO-1 fowlpox virus. *Int J Cancer*. **136**(6):E590-601.
68. de Melo, A.B., Nascimento, E.J., Braga-Neto, U., Dhalia, R., Silva, A.M., Oelke, M., Schneck, J.P., Sidney, J., Sette, A., Montenegro, S.M., and Marques, E.T. (2013) T-cell memory responses elicited by yellow fever vaccine are targeted to overlapping epitopes containing multiple HLA-I and -II binding motifs. *PLoS Negl Trop Dis*. 2013;**7**(1):e1938.
69. Zeng, G., Wang, X., Robbins, P.F., Rosenberg, S.A., and Wang, R.F. (2001) CD4(+) T cell recognition of MHC class II-restricted epitopes from NY-ESO-1 presented by a prevalent HLADP4 allele: association with NY-ESO-1 antibody production. *Proc Natl Acad Sci U SA*. **98**(7):3964-9.

Abbreviations: A2, HLA-A*0201; ANN, artificial neural network; BSP, BirA-substrate peptide; ESO, NY-ESO-1; CTL, cytotoxic T lymphocyte; PBMC, peripheral blood mononuclear cells TA; Tumor Antigen; pMHC, peptide-MHC complex, tumor antigen; TCR, T cell antigen receptor.

FIGURE LEGENDS

FIGURE 1. A2-ESO peptide binding. A. Binding of ESO peptides to A2 was assessed by peptide-driven refolding assay. The scatter blot represents five independent experiments (black dots) and their mean values and SD (red lines). The grey bars represent the mean values. The Flu MP_{58-66} peptide served as positive and no peptide as negative control. The red line indicates 30% refolding. **B.** Depicted are the principles of the refolding (top) and rebinding (bottom) assays. The A2 heavy and light chains are shown in light and dark brown, respectively, the peptide in dark blue and Cy5 in light blue. **C.** Correlation between the results of the two assays; the inserted values indicate the Pearson coefficient r and the p value.

FIGURE 2. A2-ESO peptide complex kinetic stability. A. The A2-ESO peptide complexes for which refolding efficiency was >30% were incubated at 37°C for different period of times and the complex content assessed. Half-lives were calculated and represented in hours. The scatter blot represents three independent experiments (black dots) and their mean values and SD (red lines). The grey bars represent the mean values. **B.** Correlation between measured kinetic complex stability ($\tau_{1/2}$ in h) and refolding score (% of max). The numbers designate the peptides, Flu the influenza MP_{58-66} peptide (green), p the p value and r the Pearson coefficient. Dots in blue represent peptides immunogenic in humans and mice, red dots those immunogenic only in A2 transgenic mice and black dots non-immunogenic peptides. **C.** Correlation between the NetMHC 3.4 predicted ESO peptides binding affinities (IC_{50} in nM) and NetMHCstabpan predicted complex stabilities ($\tau_{1/2}$ in h**)**. The inserted numbers and the color-coding are as in B.

FIGURE 3. Immunogenicity of ESO peptides. A. Groups of A2 transgenic, H-$2^{-/-}$ mice (n = 5) were immunized with peptide pools in IFA and CpG. After one booster immunization $CD8^+$ splenocytes were isolated and assayed for IFNγ production by ELISPOT upon stimulation with T2 cells pulsed with 1 µM of peptide. Non-specific values measured in the absence of peptide, were subtracted. Mean values and SD were calculated from two experiments. The red stars indicate peptides immunogenic in mice and humans. **B.** PBMC from ESO vaccinated patients NW 1789 and NW 3276 were stimulated once with the indicated peptide and IFNγ responses assessed by ELISPOT upon stimulation with peptide pulsed T2 cells (blue bars) or autologous DC (red bars). Non-specific responses observed in the absence of peptide, were subtracted. Mean values and SD were calculated from two experiments.

FIGURE 4. Immunogenicity of ESO peptides. A,B. Correlations between the measured refolding (x-axis; in %) (A) or A2-ESO-peptide complex kinetic stability (x-axis $\tau_{½}$ in h) (B) and the epitope score predicted by the NetTepi server (y-axis; in AU). The inserted vertical lines mark the 50% refolding score (A) or $\tau_{½}$ of

4 h and the horizontal line the NetTepi score of 0.5 AU. The numbers designate the peptides, Flu the influenza MP_{58-66} peptide (green), p the p value and r the Pearson coefficient. Dots in blue represent peptides immunogenic in humans and in mice, red dots those immunogenic only in A2 transgenic mice and black dots non-immunogenic peptides. **C.** The immunogenic peptides containing the $ESO_{159-165}$ sequence are highlighted in olive green, those containing the $ESO_{110-116}$ sequence in light green and the one containing the ESO_{87-93} sequence in grey. The numbers left indicate the peptide No, those right the peptide length and the red stars previously reported immunogenic peptides. **D.** The immunogenic peptides are represented with the potentially solvent exposed amino acids in bold; highlighted in yellow are large hydrophobic, in magenta aromatic and in grey the main A2 anchor residues. **E.** The ESO sequence with the three immunogenic core sequences highlighted as in C. The residues shown in underlined red indicate proteasomal cleavage sites as predicted by the NetChop 3.1 server (www.cbs.dtu.dk/services/NetChop/)

Table 1

No	Position[a]	Length	Sequence[a]	Affinity (nM)[b]	Stability (h)[c]	Epi score[d]	IEDB IS[e]
1	158-167	10	LLMWITQCFL	13	15.59	0.73	0.25
2	108-116	9	SLAQDAPPL	20	2.81	0.59	-0.06
3	86-94	9	RLLEFYLAM	23	4.21	0.63	0.22
4	159-167	9	LMWITQCFL	32	2.51	0.62	0.16
5	91-100	10	YLAMPFATPM	35	1.65	0.57	0.002
6	159-169	11	LMWITQCFLPV	35	7.15	0.68	0.17
7	161-169	9	WITQCFLPV	57	4.29	0.49	-0.06
8	108-118	11	SLAQDAPPLPV	69	4.45	0.59	-0.08
9	121-128	8	VLLKEFTV	112	5.53	0.63	0.02
10	126-135	10	FTVSGNILTI	172	0.97	0.42	0.01
11	86-96	11	RLLEFYLAMPF	192	2.08	0.42	0.08
12	120-128	9	GVLLKEFTV	194	0.78	0.44	-0.01
13	154-162	9	QQLSLLMWI	206	1.62	0.44	-0.21
14	110-118	9	AQDAPPLPV	229	0.54	0.37	0.009
15	91-98	8	YLAMPFAT	241	1.65	0.47	-0.03
16	157-167	11	SLLMWITQCFL	241	3.71	0.56	0.12
17	152-162	11	CLQQLSLLMWI	321	2.54	0.38	-0.36
18	86-93	8	RLLEFYLA	356	5.95	0.59	0.2
19	158-165	8	LLMWITQC	383	10.32	0.51	0.23
20	93-102	10	AMPFATPMEA	437	0.74	0.37	0.09
21	86-95	10	RLLEFYLAMP	442	0.61	0.42	0.13
22	148-156	9	SISSCLQQL	446	1.53	0.29	-0.45
23	145-153	9	LQLSISSCL	562	1.39	0.35	-0.37
24	122-132	11	LLKEFTVSGNI	760	0.81	0.37	0.09
25	157-166	10	SLLMWITQCF	771	1.19	0.29	0.07
26	162-171	10	ITQCFLPVFL	813	0.7	0.32	0.1
27	160-169	10	MWITQCFLPV	822	1.3	0.29	0.01
28	155-162	8	QLSLLMWI	831	1.49	0.39	-0.05
29	158-166	9	LLMWITQCF	949	4.22	0.38	0.2
30	162-169	8	ITQCFLPV	994	2.3	0.37	0.002
31	157-165	9	SLLMWITQC	1015	2.41	0.38	0.12
32	109-118	10	LAQDAPPLPV	1023	0.56	0.26	-0.01
33	132-140	9	ILTIRLTAA	1166	1.62	0.34	0.24
34	93-100	8	AMPFATPM	1706	0.81	0.28	0.18
35	152-160	9	CLQQLSLLM	1785	1.22	0.23	-0.34
36	146-156	11	QLSISSCLQQL	1814	0.97	0.29	-0.47
37	153-162	10	LQQLSLLMWI	1834	0.82	0.25	-0.25
38	71-80	10	GLNGCCRCGA	2380	0.98	0.28	-0.05
39	144-153	10	QLQLSISSCL	2404	0.91	0.25	-0.41
40	132-139	8	ILTIRLTA	2643	1.18	0.29	0.22
41	87-94	8	LLEFYLAM	2760	0.52	0.27	0.17

a MQAEGRGTGG STGDADGPGG PGIPDGPGGN AGGPGEAGAT GGRGPRGAGA ARASGPGGGA[60]
PRGPHGGAAS GLNGCCRCGA RGPESRLLEF YLAMPFATPM EAELARRSLA QDAPPLPVPG[120]
VLLKEFTVSG NILTIRLTAA DHRQLQLSIS SCLQQLSLLM WITQCFLPVF LAQPPSGQRR[180]

b Binding affinity (IC_{50}) predicted by NetMHC 3.4; cutt-off 3000 nM

c Complex stability ($\tau_{1/2}$) predicted by NetMHCstabpan

d T cell epitope score (AU) predicted by Netepi 1.0

e IEDB MHC I immunogenicity score (IS)

Figure 1

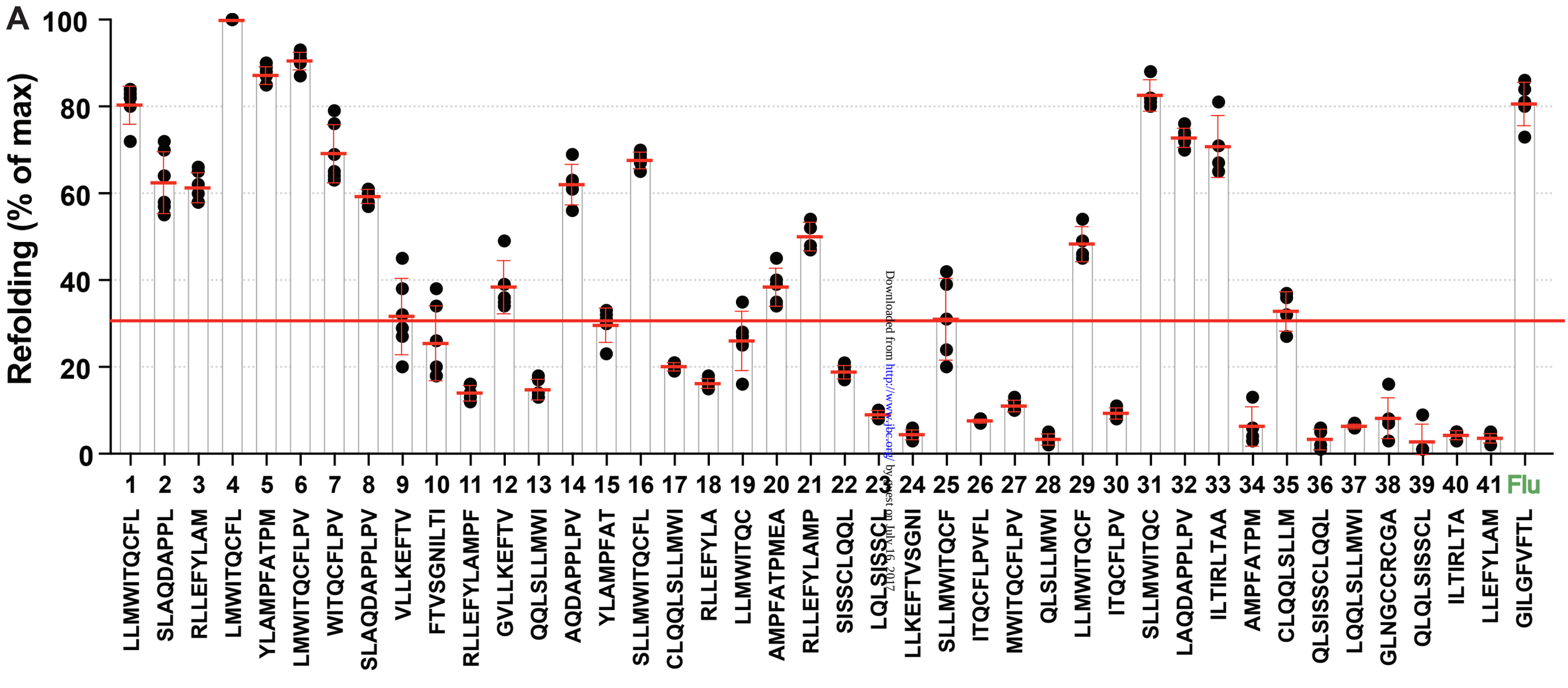

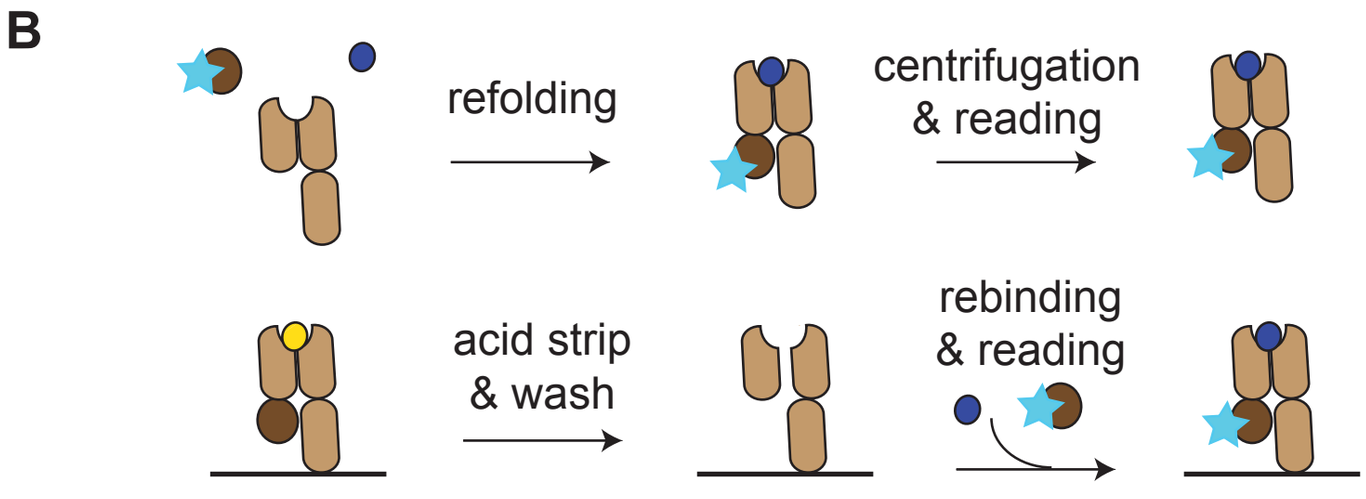

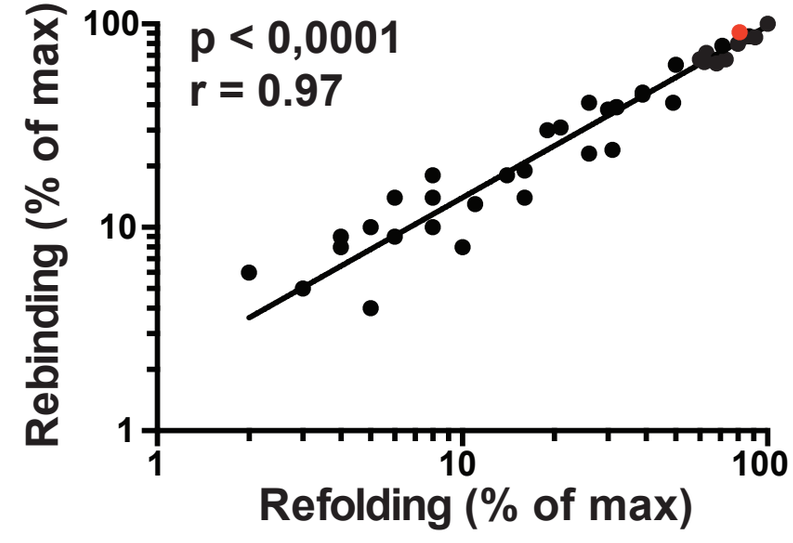

Figure 2

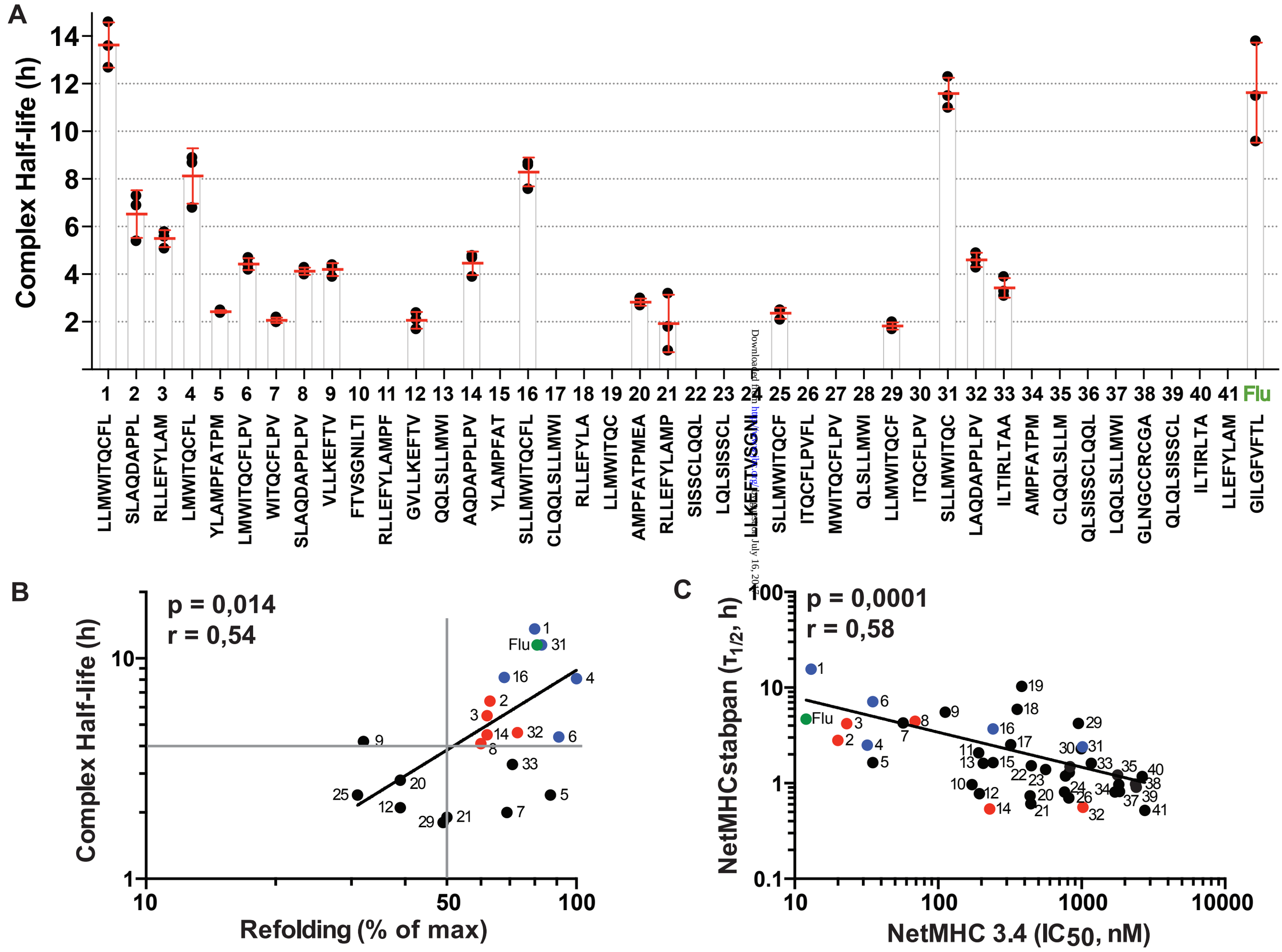

Figure 3

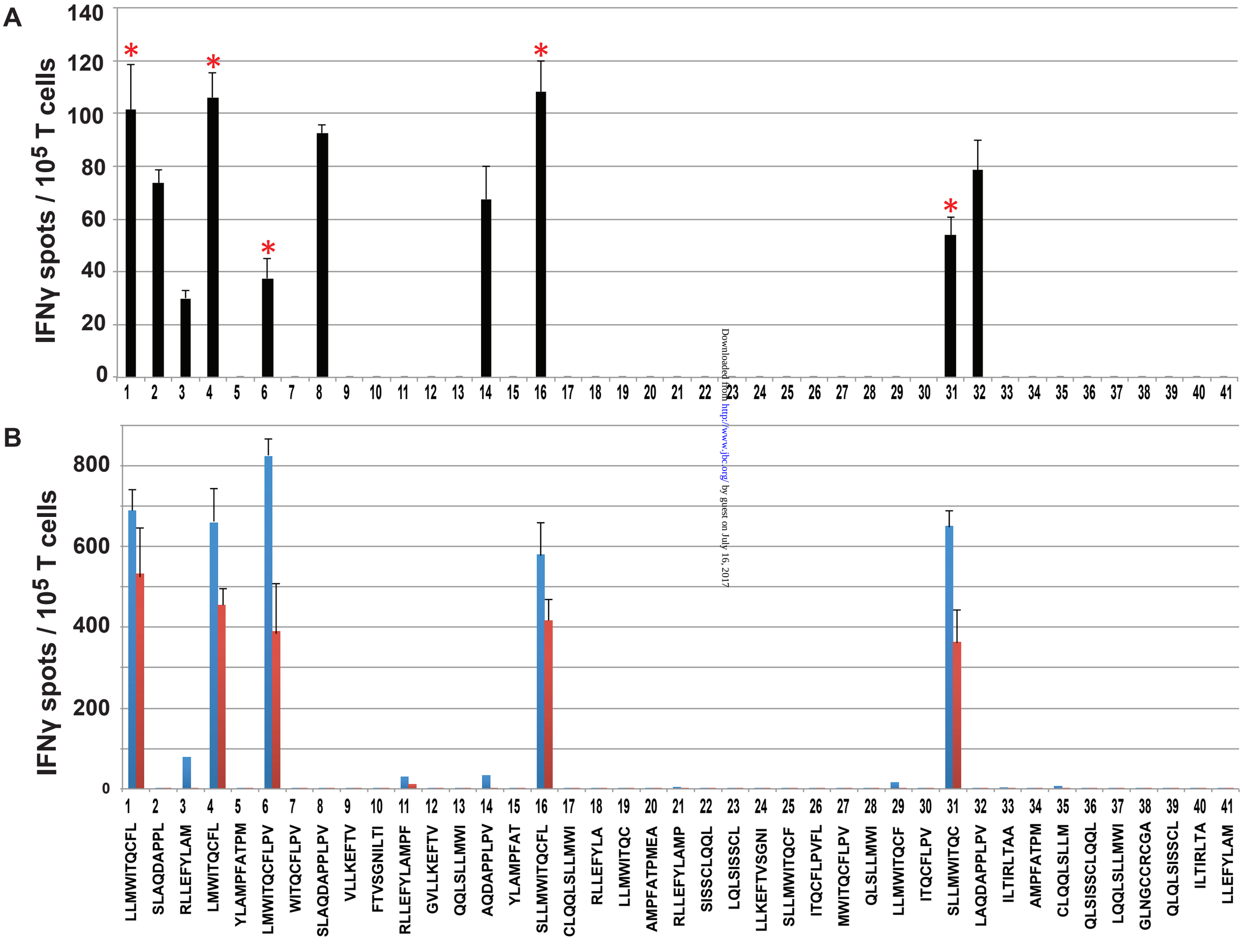

Figure 4

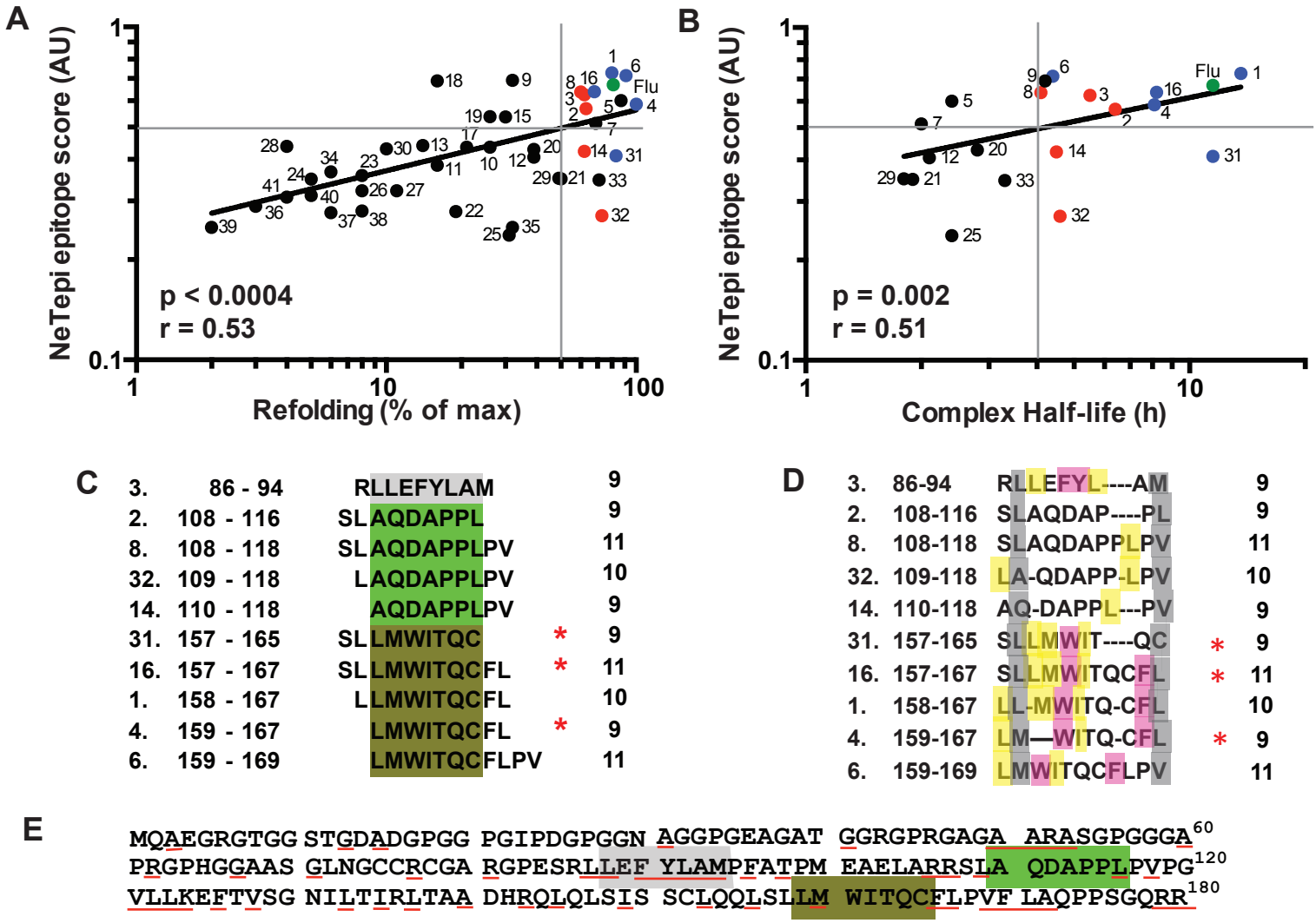
A
NeTepi epitope score (AU)
Refolding (% of max)
p < 0.0004
r = 0.53
B
NeTepi epitope score (AU)
Complex Half-life (h)
p = 0.002
r = 0.51
Flu
C
3. 86 - 94 RLLEFYLAM 9
2. 108 - 116 SLAQDAPPL 9
8. 108 - 118 SLAQDAPPLPV 11
32. 109 - 118 LAQDAPPLPV 10
14. 110 - 118 AQDAPPLPV 9
31. 157 - 165 SLLMWITQC * 9
16. 157 - 167 SLLMWITQCFL * 11
1. 158 - 167 LLMWITQCFL 10
4. 159 - 167 LMWITQCFL * 9
6. 159 - 169 LMWITQCFLPV 11
D
3. 86-94 RLLEFYL----AM 9
2. 108-116 SLAQDAP----PL 9
8. 108-118 SLAQDAPPLPV 11
32. 109-118 LA-QDAPP-LPV 10
14. 110-118 AQ-DAPPL---PV 9
31. 157-165 SLLMWIT----QC * 9
16. 157-167 SLLMWITQCFL * 11
1. 158-167 LL-MWITQ-CFL 10
4. 159-167 LM—WITQ-CFL * 9
6. 159-169 LMWITQCFLPV 11
E
MQAEGRGTGG STGDADGPGG PGIPDGPGGN AGGPGEAGAT GGRGPRGAGA ARASGPGGGA 60
PRGPHGGAAS GLNGCCRCGA RGPESRLLEF YLAMPFATPM EAELARRSLA QDAPPLPVPG 120
VLLKEFTVSG NILTIRLTAA DHRQLQLSIS SCLQQLSLLM WITQCFLPVF LAQPPSGQRR 180

In silico and cell-based analyses reveal strong divergence between prediction and observation of T cell recognized tumor antigen T cell epitopes

Julien Schmidt, Philippe Guillaume, Danijel Dojcinovic, Julia Karbach, George Coukos and Immanuel Luescher

J. Biol. Chem. published online May 23, 2017
